International Journal of Trend in Scientific Research and Development (IJTSRD)
Volume 9 Issue 5, Sep-Oct 2025 Available Online: www.ijtsrd.com e-ISSN: 2456 – 6470

UV–Vis and FTIR Spectroscopic Analysis of YBCO Superconductors with Different Yttrium Concentrations

Mozdlifa Bayin Mohamed[1], Mahmoud Hamid Mahmoud Hilo[2], Ahmed Abubaker Mohamed[3]

[1,2]Sudan University of Science and Technology, Khartoum, Sudan
[3]Al-Ayen University, Dhi Qar Governorate, Iraq

ABSTRACT

This study investigates the effect of varying yttrium content on the structural and optical properties of $YBa_2Cu_3O_{7-\delta}$ (YBCO) superconductors synthesized via the chemical extenuation method. Three compositions—$Y_{1.00}Ba_2Cu_3O_7$, $Y_{0.90}Ba_2Cu_3O_7$, and $Y_{0.80}Ba_2Cu_3O_7$—were characterized using Fourier Transform Infrared (FTIR) and UV-Visible (UV-Vis) spectroscopy. FTIR analysis revealed that decreasing Y content resulted in Cu–O bond weakening, increased oxygen vacancies, and pronounced lattice distortions. UV-Vis results indicated that all samples exhibited strong UV absorption, with reduced Y content enhancing absorbance, transmittance, and reflectance in specific regions. The optical band gap decreased from 1.0 to 0.8 Y-content samples, correlating with changes in electronic structure and defect states. Optical, dielectric, and conductivity measurements confirmed that Y-content tuning significantly influences charge carrier dynamics and potential superconducting performance. These findings highlight the role of yttrium concentration in tailoring YBCO properties for superconducting and optoelectronic applications.

KEYWORDS: *YBCO Superconductor, Yttrium Concentration, FTIR, UV-VIS, Superconducting Properties.*

How to cite this paper: Mozdlifa Bayin Mohamed | Mahmoud Hamid Mahmoud Hilo | Ahmed Abubaker Mohamed "UV–Vis and FTIR Spectroscopic Analysis of YBCO Superconductors with Different Yttrium Concentrations" Published in International Journal of Trend in Scientific Research and Development (ijtsrd), ISSN: 2456-6470, Volume-9 | Issue-5, October 2025, pp.75-84, URL: www.ijtsrd.com/papers/ijtsrd97434.pdf

IJTSRD97434

Copyright © 2025 by author (s) and International Journal of Trend in Scientific Research and Development Journal. This is an Open Access article distributed under the terms of the Creative Commons Attribution License (CC BY 4.0) (http://creativecommons.org/licenses/by/4.0)

INTRODUCTION

Spectroscopic techniques are essential analytical tools for probing the structural, electronic, and vibrational properties of materials. Among these, ultraviolet–visible (UV–Vis) spectroscopy and Fourier transform infrared (FTIR) spectroscopy are widely employed due to their complementary capabilities in characterizing electronic transitions and molecular vibrations, respectively [1–3].

UV–Vis spectroscopy measures the absorption of ultraviolet and visible light by a sample, typically in the wavelength range of 190–900 nm [4,5]. The technique is primarily used to investigate electronic transitions between molecular orbitals, providing insights into band gap energies, chromophoric groups, and the concentration of absorbing species through the Beer–Lambert law [6]. It is extensively applied in material science, chemistry, and biological systems for both qualitative and quantitative analysis [4].

FTIR spectroscopy, on the other hand, records the infrared absorption spectrum of a sample, typically in the mid-infrared range (4000–400 cm^{-1}), using an interferometer and Fourier transform algorithms [2,7]. The resulting spectrum provides a molecular fingerprint, enabling the identification of functional groups and monitoring of chemical bonding changes [8]. In solid-state physics and materials research, FTIR is particularly valuable for analyzing lattice vibrations, chemical composition, and structural changes during synthesis or processing [3,7,9].

When used in combination, UV–Vis and FTIR spectroscopy offer a more comprehensive understanding of material properties. UV–Vis can reveal information about electronic band structures and optical properties, while FTIR provides detailed insight into vibrational and bonding characteristics [1,3,8]. This synergy is particularly important in advanced materials research, such as thin films, nanostructures, and superconductors, where both electronic and vibrational characteristics are critical for performance evaluation [5,7,10].

Materials and Methods:

Materials:

The starting reagents included Yttrium oxide (Y_2O_3, white powder), Barium carbonate ($BaCO_3$), Copper(II) oxide (CuO, black powder), diluted sulfuric acid (40%), distilled water, and acetone. All reagents were of analytical grade and used without further purification.

Stoichiometry and Sample Preparation:

The desired superconducting phase, $YBa_2Cu_3O_7$, was synthesized according to the following reaction:

$$\frac{1}{2}Y_2O_3 + 2BaCO_3 + 3CuO \rightarrow YBa_2Cu_3O_7 + 2CO_2\uparrow$$

Initial weights for a 1 g sample were calculated as: Y_2O_3 (0.151 g), $BaCO_3$ (0.529 g), and CuO (0.320 g). To increase yield, each reagent mass was multiplied by a factor of three. Three different samples were prepared to investigate the effect of varying Y_2O_3 content (100%, 90%, and 80% nominal levels). The calculated quantities are presented below:

Sample 1 (100% Y_2O_3):
Y_2O_3: 0.151 g × 3 = 0.453 g
$BaCO_3$: 0.529 g × 3 = 1.587 g
CuO: 0.320 g × 3 = 0.960 g

Sample 2 (90% Y_2O_3):
Y_2O_3: 0.1359 g × 3 = 0.4077 g
$BaCO_3$: 0.529 g × 3 = 1.587 g
CuO: 0.320 g × 3 = 0.960 g

Sample 3 (80% Y_2O_3):
Y_2O_3: 0.1208 g × 3 = 0.3624 g
$BaCO_3$: 0.529 g × 3 = 1.587 g
CuO: 0.320 g × 3 = 0.960 g

Cleaning Procedure:

Prior to use, the mortar and pestle were cleaned sequentially to avoid contamination. The cleaning steps included: rinsing with tap water, immersion in 40% diluted sulfuric acid, drying, washing with distilled water, and finally rinsing with acetone.

Synthesis Process:

For **Sample 1**, the dry mixture of Y_2O_3, $BaCO_3$, and CuO was ground in a mortar with gentle clockwise motion for 30 minutes until a homogeneous grey powder was obtained. The powder was transferred into a high-temperature-resistant crucible and calcined in a carbolated furnace at **850 °C** for 1 hour. After cooling to room temperature, the black mixture was reground with the addition of acetone for 30 minutes, then subjected to a second calcination at **850 °C** for 5 hours. Finally, the resulting hard, sintered mass was cooled to room temperature and ground again for 30 minutes before subsequent analysis.

Sample 2 and **Sample 3** were prepared following the same procedure, using adjusted Y_2O_3 quantities corresponding to 90% and 80% nominal content, respectively.

Results and discussion:

FTIR results:

The FTIR spectra of YBCO were studied with different Y content ($Y_{1.00}Ba_2Cu_3O_7$, $Y_{0.90}Ba_2Cu_3O_7$, and $Y_{0.80}Ba_2Cu_3O_7$), comparing Cu-O and Y-O vibrations, structural changes, and the implications of these changes on superconducting properties.

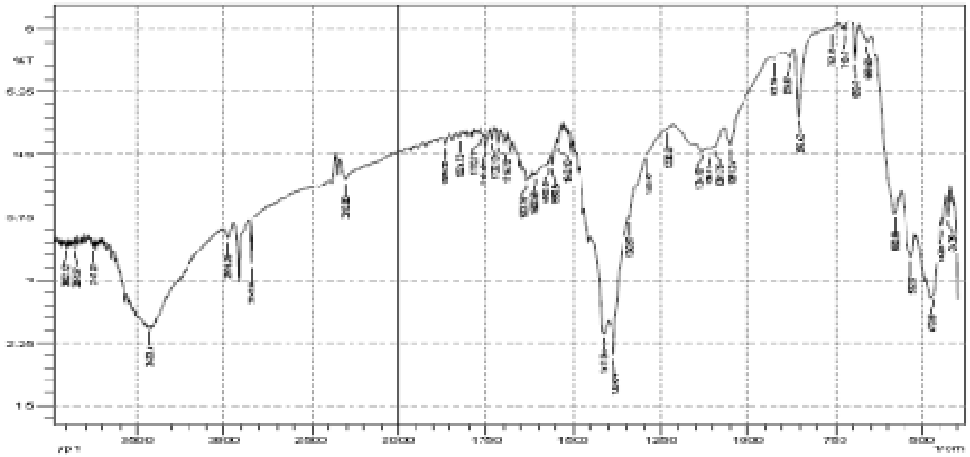

Fig. (1) FTIR spectrum of $Y_{1.00}Ba_2Cu_3O_7$

The well-defined FTIR spectrum of $Y_{1.00}Ba_2Cu_3O_7$ shows excellent stoichiometric composition. Cu-O stretching and bending vibrations within 450-600 cm^{-1} reflect strong bonding and a well-formed superconducting phase. Cu-O chains are very important in supplying charge carriers to the CuO_2 planes. The Ba-O and Y-O vibrations within the range of 200-400 cm^{-1} depict the structural stability of the perovskite lattice. The absence of peak broadening and contaminants reflects excellent phase purity and crystallinity.

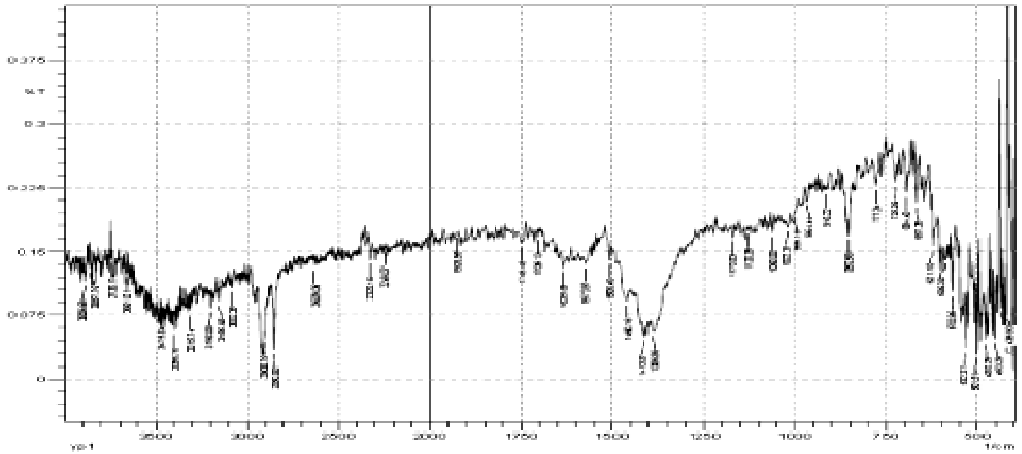

Fig. (2) FTIR spectrum of $Y_{0.90}Ba_2Cu_3O_7$

The FTIR spectrum of $Y_{0.90}Ba_2Cu_3O_7$ reflects moderate departures from its ideal form and reveals structural variations with a low concentration of Y. The minor shifting of Cu-O stretching vibrations towards lower wavenumber positions signifies weakened Cu-O bonding and partial oxygen vacancies within the Cu-O chains. Peak broadening, as such, reflects the increase in lattice distortions. Consequently, the characteristic vibrations of the Y-O band in the frequency region 200-400 cm^{-1} appeared with relatively reduced intensity to reveal partial instability or substitutional effects. Despite these changes, the fundamental natures of the Ba-O vibrations in no way change.

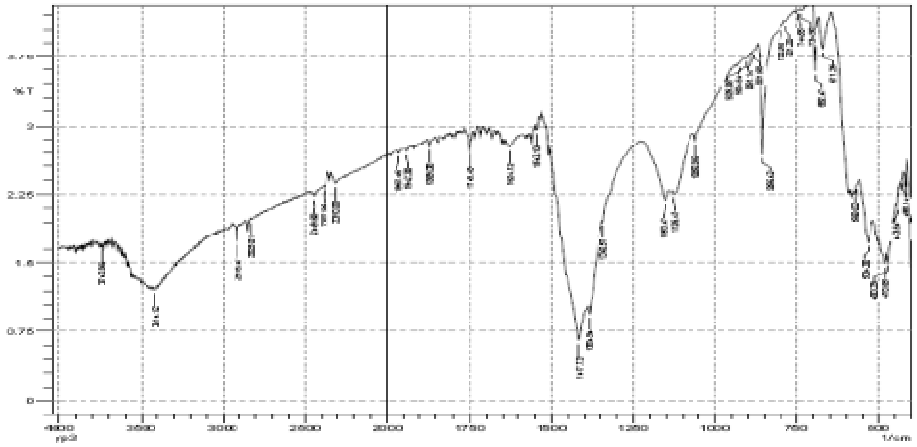

Fig. (3) FTIR spectrum of $Y_{0.80}Ba_2Cu_3O_7$

The FTIR spectrum of $Y_{0.80}Ba_2Cu_3O_7$ is seriously deviated, indicating a structural change by the decrement of Y content. A great shifting of the Cu-O stretching vibration to the lower wavenumber indicates a further weakening of the Cu-O bonds and increased oxygen vacancies. Strong broadening of peaks evidences a higher degree of lattice disorder. With this, the strength of Y-O vibrations in the range of 200-400 cm^{-1} reduces tremendously, indicating low occupancy at Y-sites and, hence, structural instabilities.

Table (1) Comparative of FTIR Spectra for Different Y Content.

Sample	Cu-O Peak Position	Peak Broadening	Oxygen Deficiencies	Structural Stability
$Y_{1.00}Ba_2Cu_3O_7$	Sharp, well-defined (450–600 cm^{-1})	Minimal	No significant vacancies	High
$Y_{0.90}Ba_2Cu_3O_7$	Slight shift to lower wavenumbers	Moderate	Some vacancies in CuO chains	Slightly distorted
$Y_{0.80}Ba_2Cu_3O_7$	Pronounced shift to lower wavenumbers	Significant	High vacancy concentration	Considerably distorted, possible secondary phases

UV-VIS results:

The UV-VIS spectrometer was used to record the absorbance spectrum of YBCO with different Y content, and then the other optical properties were calculated.

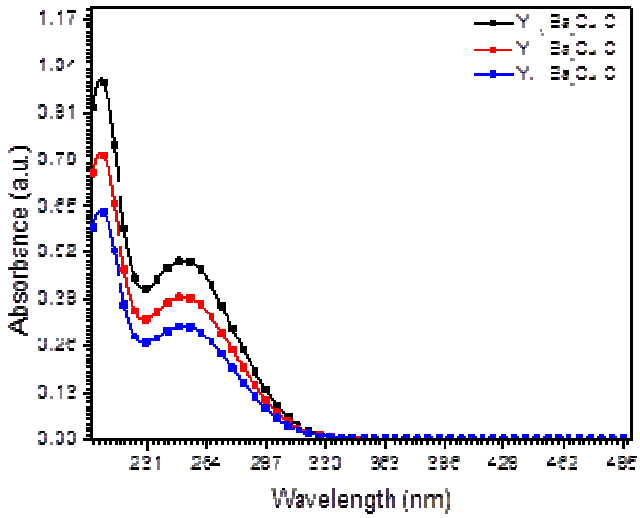

Fig (4) the absorbance of YBCO with different Y content

The YBCO absorbance spectrum, with variable Y content, shown in Fig (---), provides useful information about the optical properties of the material. Light absorption plotted as a function of wavelength varies significantly depending on the Y composition.

In the UV range, absorbance for all samples was very high, indicating strong electronic transitions, most likely caused by charge transfer mechanisms in the YBCO structure. It is observed that the sample with lower Y content ($Y_{0.80}Ba_2Cu_3O_7$) has a higher absorbance than the others ($Y_{0.90}Ba_2Cu_3O_7$ and $Y_{1.00}Ba_2Cu_3O_7$), and decreasing in the Y content improves the light absorption. This may be due to the changing electronic structure of the material, which provides a greater density of states now available for optical transitions.

While the wavelength increases, the absorbance declines gradually, reflecting strong UV absorption up to less absorption in the visible and near-infrared range. The occurrence of several peaks underlines the interactions of electronic states, possibly due to the effects of crystal structure and defects caused by variations in Y concentration.

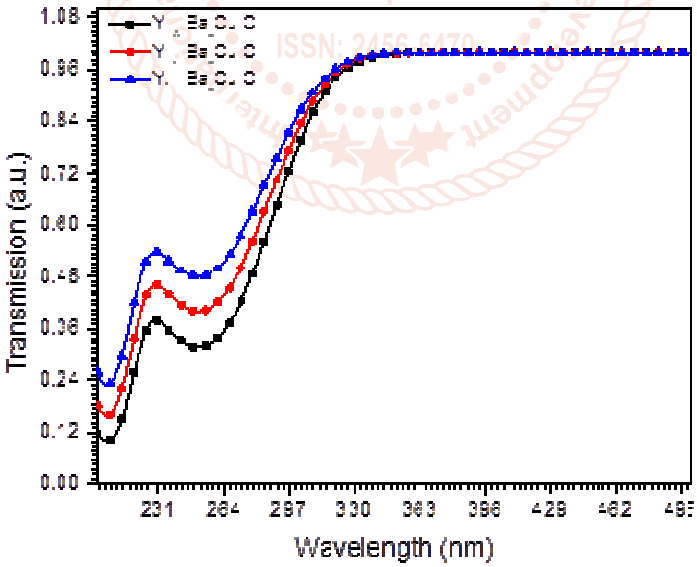

Fig (5) the transmission of YBCO with different Y content

From the fig (5), one can find that the YBCO with variable Y concentration gives information about optical transparency and interactions with light in different wavelengths. The Y content changing the transmittance spectrum achieved via a graphical plot may set out data that belongs to these properties of such material. All samples show very low transmission at the lower wavelengths, indicating high absorption in this region. This agrees with the electronic transitions taking place in the absorbance spectra, which involve significant charge transfer between Cu and O in the YBCO lattice. However, at longer wavelengths, transmission starts to increase substantially, reflecting the transition from severe absorption to increased transparency within the visible and near-infrared regions.

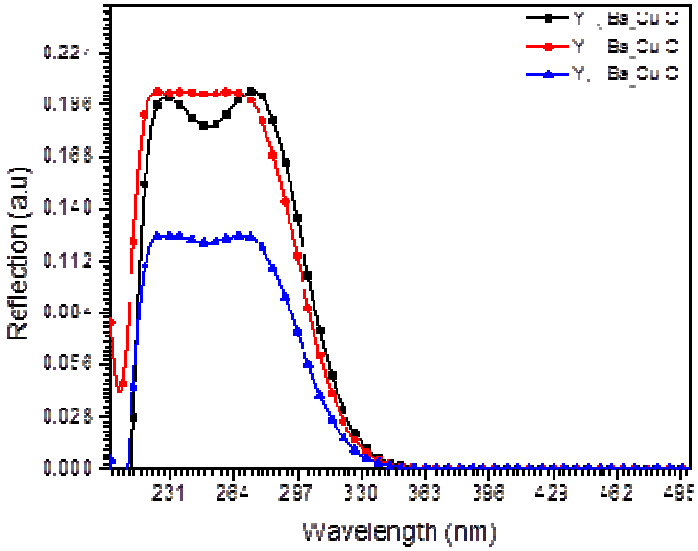

Fig (6) the reflection of YBCO with different Y content

Fig (6) shows the reflection spectrum of YBCO with variable Y content and gives important information about how this material interacts with incident light; it can be calculated according to the law of energy conservation and by knowing the value of each transmittance(T) and Absorbance (A).

$$R + T + A = 1$$

In the lower wavelength area, UV, all sample curves start with low reflectance, which means strong absorption of incident light. While increasing the wavelength, a dramatic increase in reflection is noticed, indicating a transition in which the material starts reflecting most of the light instead of absorbing it. In this region, $Y_{0.8}Ba_2Cu_3O_7$, which represents lower Y content, has a higher reflectance compared to the other samples, showing that decreasing Y content improves the material's reflectivity.

A notable plateau is realized at the middle-wavelength range, where the reflectance is rather stable before it starts to decline at higher wavelengths. The difference in the plateau levels of all curves suggests that the optical properties of YBCO are influenced by the Y concentration, likely due to changes in the electronic structure and surface characteristics of the material. This difference may be due to the difference in oxygen vacancies, lattice distortions, or charge carrier density, as all can affect the reflectivity of the material. As the wavelength extends to the near-infrared region, the reflectance decreases gradually and moves close to a minimum. It therefore follows that in such a long-wavelength regime, the material becomes less reflective, and as a result, more light is transmitted or absorbed.

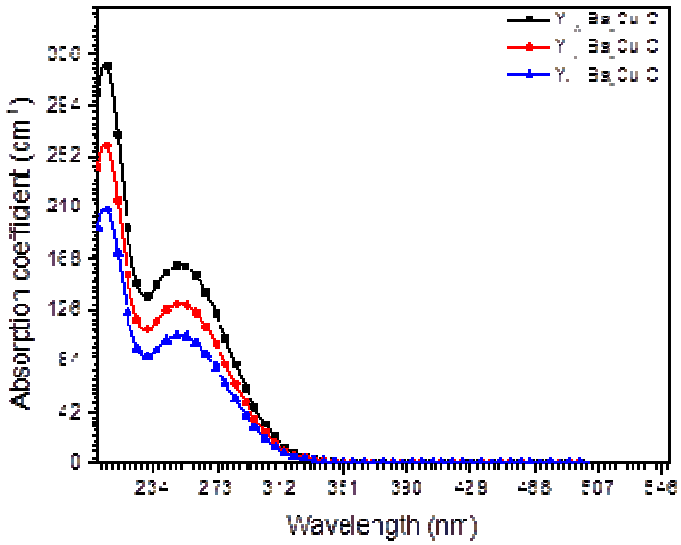

Fig (7) the absorption coefficient of YBCO with different Y content

The absorption coefficient (α) of YBCO with different Y content is shown in Fig (---) and Fig (4.12), it can be obtained from the following relation.

$$\alpha = \frac{2.303 \times A}{t}$$

Where (A) is the absorbance and (t) is the optical length in the samples. At short wavelengths, both curves have a sharp peak, while the absorption is particularly strong, hence showing high interaction between incident photons and the electronic states in the material. $Y_{0.8}Ba_2Cu_3O_7$ shows an even more pronounced peak in absorption compared to the other samples. It means that, with the decrease in Y content, the absorption of high-energy photons increases owing to modifications within the electronic band structure, such as variation of energy gap or defect states. With the increasing wavelength, the absorption coefficient reduces gradually, and all samples exhibit a wide absorption peak. The region is ascribed to the transitions of different energy states in the material. The intensity of absorption in this region is slightly stronger, $Y_{0.8}Ba_2Cu_3O_7$, which suggests that the content of Y influences the optical absorption properties of the material. The appearance of these absorption features can be due to electronic transitions related to oxygen vacancies, Cu-O bond interactions, or structural distortions introduced by Y substitution. At longer wavelengths, all samples stabilize at extremely low absorption coefficients. This shows that the material becomes more transparent in the infrared range.

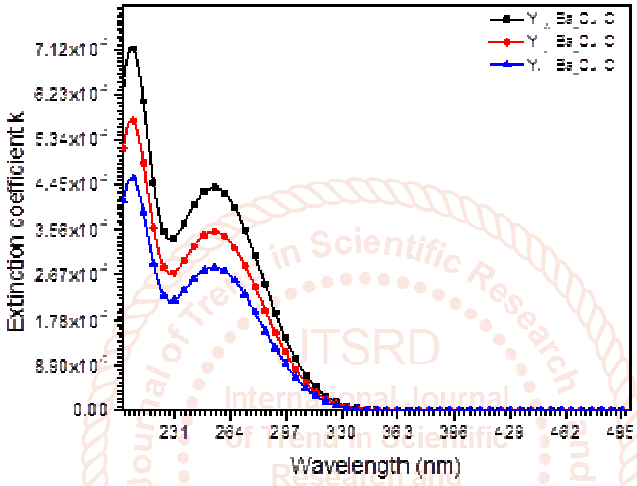

Fig (8) the extinction coefficient of YBCO with different Y content

The variation of the extinction coefficient (K) values of YBCO with different Y content samples as a function of (λ) was shown in Fig (---), it can be estimated through the relation

$$k = \frac{\alpha\lambda}{4\pi}$$

Extinction coefficient, k, versus wavelength and Y-content in YBCO characterizes the optical absorption in YBCO. Indeed, strong absorptions below 300 nm were noted in the UV region and exhibited a larger peak for a higher Y-content due to an electronic structure or defect states. In the 300-600 nm range, several peaks indicate the interactions of charge carriers and interband transitions; absorption remains a bit higher for decreased Y content. For longer wavelengths (> 600 nm, infrared region), the extinction coefficient is much lower, reflecting transparency in the infrared spectrum.

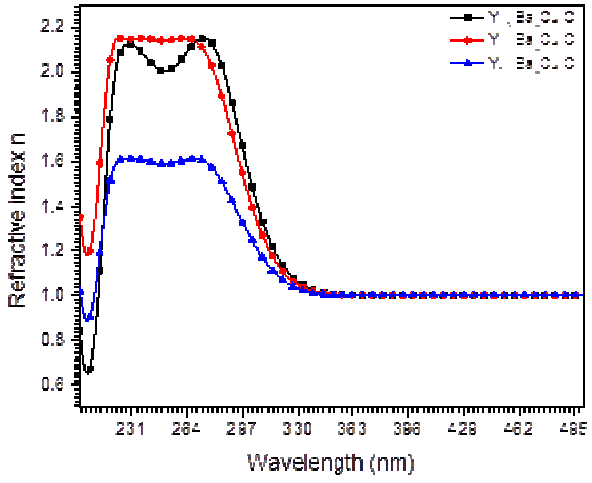

Fig (9) the refractive index of YBCO with different Y content

Fig (9) represents the YBCO refractive index with different Y contents. The refractive index, among the basic optical properties of this material, prescribes how a light signal navigates within that material; furthermore, properties based upon this quantity comprise reflectivity, transmission, and phase velocity. Changes in such a parameter could be enlightening concerning understanding its optical behavior or electronic structure. The value of n was calculated from the equation:

$$n = \left[\left(\frac{(1+R)}{(1-R)}\right)^2 - (1+k^2)\right]^{\frac{1}{2}} + \frac{(1+R)}{(1-R)}$$

Where (R) is the reflectivity. In the UV region, particularly below 300 nm, all samples show a sharp increase in the refractive index before it reaches a maximum and then stabilizes. Compared to $Y_{0.8}Ba_2Cu_3O_7$, the other samples indicate a lower Y content, demonstrating that decreased Y content will enhance optical interactions in the UV range. This effect is most probably due to electronic transitions or interband absorption within this spectral range.

Within the visible spectrum (300–600 nm), the refractive index remains almost constant, revealing a plateau. In this range, the $Y_{0.8}Ba_2Cu_3O_7$ keeps values higher than the other samples, suggesting that Y content affects the optical properties of YBCO in visible light. Such stability of the refractive index in this region presumes that YBCO may act as a dielectric material with minimal changes in optical response and thus may be applied in cases requiring consistent refractive properties. Above 600 nm and especially beyond that in the infrared IR, the two curves continuously decrease to reach a flat tail. Such a decreasing trend would imply that the YBCO becomes increasingly transparent to IR, with reduced absorption and dispersion in that region.

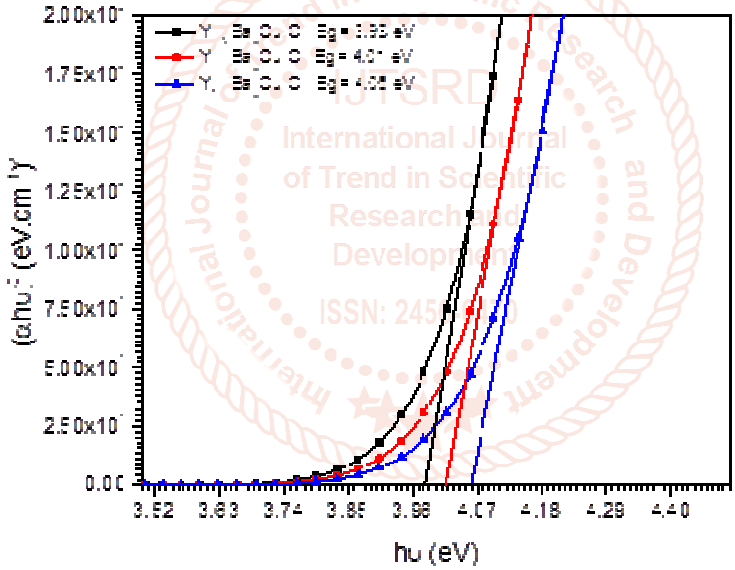

Fig (10) the optical energy band gap of YBCO with different Y content

The optical energy gap (Eg) of YBCO with different Y content samples has been calculated using the Tauc equation:

$$(\alpha h\upsilon)^2 - C(h\upsilon - Eg)$$

The x-axis is for the photon energy (hν), while the y-axis is for $(\alpha h\nu)^2$, with α being the absorption coefficient. The extension of the linear part of each curve to cut the energy axis gives the value of the optical band gap. Fig (--) shows that as the Y content increases, the optical energy band gap increases. The increased band gap for higher substitution of Y is because of changes in electronic structure and oxygen stoichiometry, including a reduction in carrier density, which decreases the available electronic states around the Fermi level. One more reason for such a shift in conduction and valence bands could be the enhanced localization of the charge carriers. Besides, lattice structural changes due to Y substitution may further cause changes in the electron-lattice interactions and, hence, affect the band structure. This band gap tunability is highly significant for the realization of this material both in superconducting and optoelectronic applications. Reduced Y content, Y=0.8 (smaller band gap), favors applications requiring efficient charge transport, such as conductive coatings and infrared detection. The higher Y content, Y=1.0 (larger band gap), is better suited for high-energy optical devices, transparent conductive oxides, and applications involving reduced free carrier absorption.

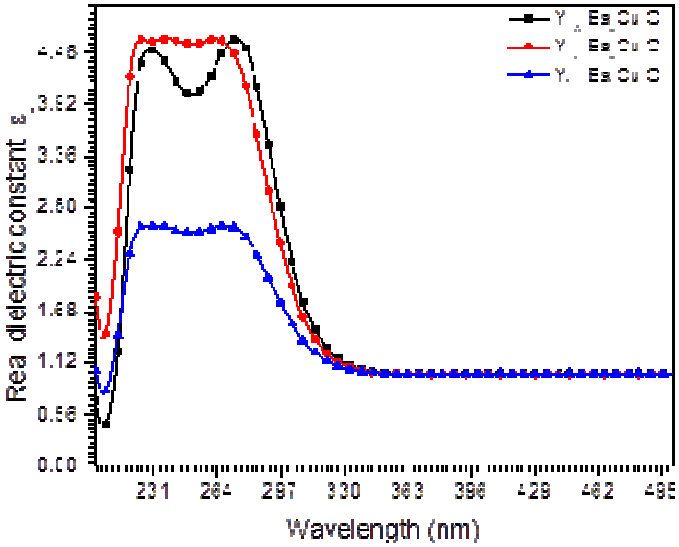

Fig (11) the real dielectric constant of YBCO with different Y content

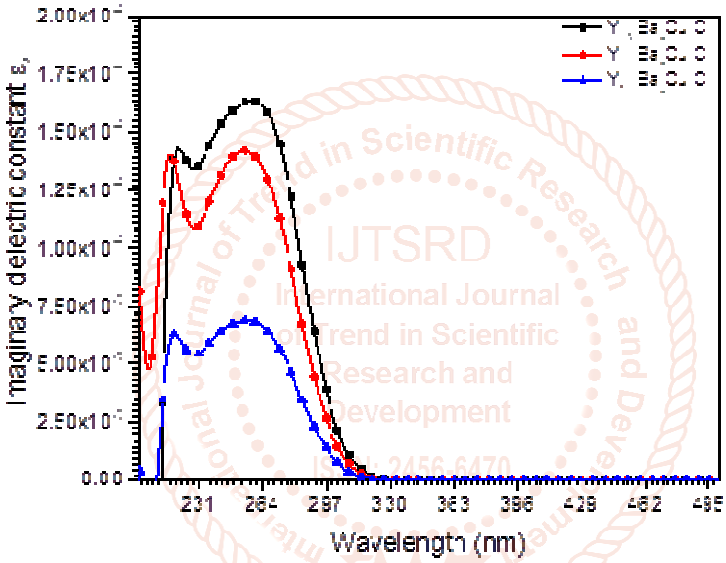

Fig (12) the imaginary dielectric constant of YBCO with different Y content

The dielectric constant characterizes the capability of a material to store electrical energy in an electric field it can be calculated from the relation.

$$\varepsilon_1 = n^2 - k^2 \; \varepsilon_2 = 2nK$$

Fig (--) and Fig (--) represent the real and imaginary dielectric constants of YBCO with different Y content. The real part of the dielectric constant corresponds to the capability of the material for storing the electrical energy, while the imaginary one corresponds to dielectric losses and dissipation of energy. Both of the parameters have great importance from the viewpoint of the electrical and superconducting behavior of YBCO.

The real dielectric constant shows a peak, indicating phase transition or structural modification. For $Y_{1.00}Ba_2Cu_3O_7$, the dielectric constant is higher than that for the other samples, suggesting that Y content influences the polarizability and dielectric response of the material. The variation in charge carrier concentration, structural distortions, or oxygen content might be a reason for such variation. The curve of the imaginary dielectric constant has several peaks; these are indicative of energy dissipation due to dielectric relaxation mechanisms. More pronounced dielectric losses are represented by the $Y_{1.00}Ba_2Cu_3O_7$, which has been obtained for higher Y content and, therefore, increased energy dissipation.

Optical conductivity is one of the fundamental characteristics of materials that describe the response of a material against an externally applied electromagnetic field, mainly in the optical frequency range (infrared to ultraviolet). Using the following relation:

$$\delta_{opt} = \frac{\alpha nc}{4\pi}$$

Where (c) is the light velocity.

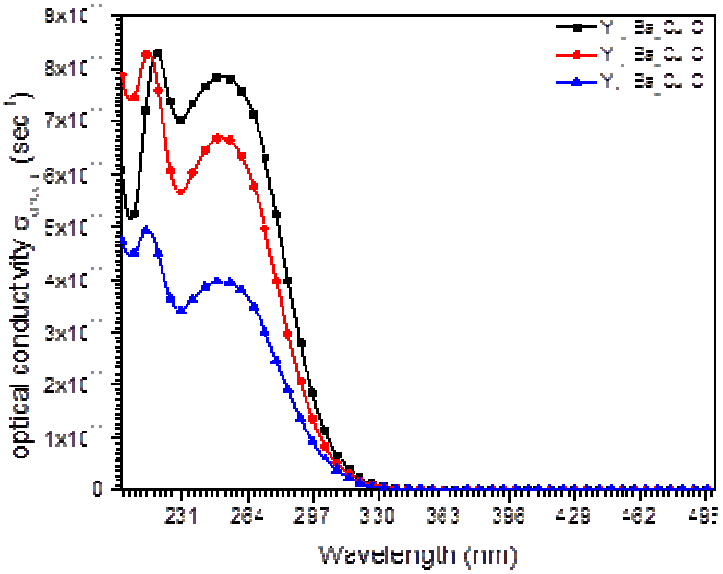

Fig (13) the optical conductivity of YBCO with different Y content

The optical conductivity of YBCO, with variation in the Y content, reflects drastic differences in both charge carrier behavior and electronic structure. The $Y_{0.80}Ba_2Cu_3O_7$ shows higher conductivity of the material because of more free carriers or lesser scattering. Correspondingly, from $Y_{1.00}Ba_2Cu_3O_7$, one gets lower conductivity since the carriers will be more localized. These indeed verify the superconducting behavior of all three at low frequencies, with the difference in peak intensities reflecting a change in carrier dynamics. For all three, conductivity declines as frequency increases from free-carrier-like conduction to interband excitations.

Electrical conductivity is defined as the measure of a material's ability to allow the flow of electric charge when an electric field is applied; it can be estimated using the following relation.

$$\delta_{elc} = \frac{2\lambda\delta_{opt}}{\alpha}.$$

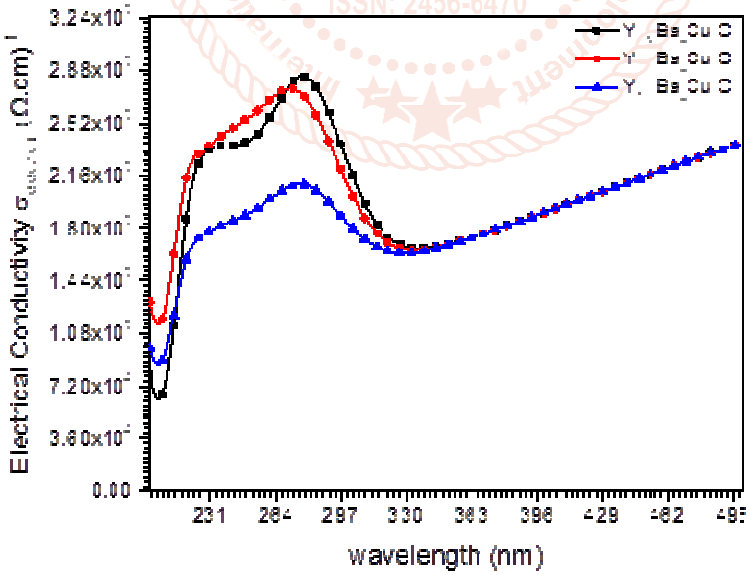

Fig (14) the electrical conductivity of YBCO with different Y content

The electrical conductivity spectra of YBCO, presented in Fig (---) for three varying levels of Y content, demonstrate considerable variation in charge transport behavior.

At lower frequencies, all the samples exhibit a broad response in conductivity, with $Y_{0.90}Ba_2Cu_3O_7$ having the highest, followed by $Y_{0.80}Ba_2Cu_3O_7$ and $Y_{1.00}Ba_2Cu_3O_7$. This shows that the $Y_{0.90}Ba_2Cu_3O_7$ contains the most mobile charge carriers and less scattering effects and, hence, exhibits higher electrical conductivity. $Y_{1.00}Ba_2Cu_3O_7$, on the other hand, is for the sample with the lowest conductivity, which indicates larger

localization effects or charge carrier scattering. The $Y_{0.80}Ba_2Cu_3O_7$ falls between the two, corresponding to intermediate electrical transport properties. As frequency increases, conductivity decreases across all samples, indicating a shift from free-carrier-dominated conduction to interband electronic excitations. The $Y_{0.80}Ba_2Cu_3O_7$ and $Y_{0.90}Ba_2Cu_3O_7$ show a more progressive reduction, but the $Y_{1.00}Ba_2Cu_3O_7$ decreases faster, demonstrating differences in how charge carriers interact with the lattice structure. However, at higher frequencies, the $Y_{0.80}Ba_2Cu_3O_7$ and $Y_{0.90}Ba_2Cu_3O_7$ begin to rise, indicating the activation of secondary conduction processes like phonon-assisted transport or localized state contributions.

Conclusion:

The experimental analysis demonstrates that yttrium concentration plays a crucial role in determining the structural stability, optical characteristics, and electrical performance of YBCO superconductors. FTIR spectra confirmed that lowering Y content increases lattice disorder and oxygen deficiencies, particularly in Cu–O chains, which are essential for charge carrier transport. UV-Vis measurements showed that reduced Y content enhances UV absorption and modifies transmittance and reflectance behaviors, while narrowing the optical band gap. Dielectric constant variations and conductivity results further indicated that lower Y content can improve optical conductivity but may compromise lattice stability. These findings suggest that precise control of Y concentration \allows optimization of YBCO materials for specific applications, balancing high conductivity with structural integrity in both superconducting and optoelectronic devices.

Recommendations:

YBCO (Yttrium Barium Copper Oxide) is considered an effective material for the fabrication of superconducting thin films

due to its excellent superconducting properties and high critical temperature.

Abbreviations:

YBCO: Yttrium Barium Copper Oxide.

XRD: X-ray diffraction.

FTIR: Fourier transform infra-red

References:

[1] Singh, A., Kumar, V., & Sharma, R. (2023). Investigation of lattice distortion and oxygen vacancies in YBCO superconductors by FTIR spectroscopy. *Physica C: Superconductivity and its Applications*.

[2] Coates, J. (2000). Interpretation of infrared spectra, a practical approach. In R. A. Meyers (Ed.), *Encyclopedia of Analytical Chemistry* (pp. 10815–10837). Chichester: John Wiley & Sons.

[3] Wang, Y., Zhao, J., & Liu, H. (2022). FTIR and UV–Vis spectroscopic analysis of perovskite oxide nanomaterials. *Spectrochimica Acta Part A: Molecular and Biomolecular Spectroscopy*

[4] Griffiths, P. R., & de Haseth, J. A. (2007). *Fourier Transform Infrared Spectrometry* (2nd ed.). Hoboken: John Wiley & Sons. https://doi.org/10.1002/047010631X

[5] Stuart, B. (2004). *Infrared Spectroscopy: Fundamentals and Applications*. Chichester: John Wiley & Sons.

[6] Hollas, J. M. (2004). *Modern Spectroscopy* (4th ed.). Chichester: John Wiley & Sons.

[7] Pavia, D. L., Lampman, G. M., & Kriz, G. S. (2015). *Introduction to Spectroscopy* (5th ed.). Boston: Cengage Learning.

[8] Skoog, D. A., Holler, F. J., & Crouch, S. R. (2018). *Principles of Instrumental Analysis* (7th ed.). Boston: Cengage Learning.

[9] Yang, H., & Griffiths, P. R. (2002). Quantitative analysis of pharmaceutical products by FTIR spectrometry. *Applied Spectroscopy*, 56(12), 1601–1608.

[10] Karabudak, E., & Gasanly, N. M. (2012). Optical properties of layered GaSe crystals studied by transmission and reflection spectroscopy. *Optics Communications*, 285(3), 410–414. https://doi.org/10.1016/j.optcom.2011.10.009